Directed transport in quantum star graphs

Jambul Yusupov

Turin Polytechnic University in Tashkent, 17 Niyazov Street, 100095 Tashkent, Uzbekistan

Maxim Dolgushev, Alexander Blumen, and Oliver Mülken

Physikalisches Institut, Universität Freiburg, Hermann-Herder-Straße 3, 79104 Freiburg, Germany

(Dated: June 29, 2021)

We study the quantum dynamics of Gaussian wave packets on star graphs whose arms feature each a periodic potential and an external time-dependent field. Assuming that the potentials and the field can be manipulated separately for each arm of the star, we show that it is possible to manipulate the direction of the motion of a Gaussian wave packet through the bifurcation point by a suitable choice of the parameters of the external fields. In doing so, one can achieve a transmission of the wave packet into the desired arm with nearly 70% while also keeping the shape of the wave packet approximately intact. Since a star graph is the simplest element of many other complex graphs, the obtained results can be considered as the first step to wave packet manipulations on complex networks.

I. INTRODUCTION

Recent experimental advances have led to very precise manipulations of atoms in optical lattices [1] and of wave packets in waveguide arrays [2, 3]. Fundamental effects such as Bloch oscillations for wave packets in tilted lattices have been experimentally confirmed by several groups [4–7]. Moreover, it has been shown that coherent control over the wave packets is possible by varying the external field: Such variations can be discrete [8, 9] or continuous [10–13]. In a two-dimensional lattice, one can achieve arbitrary displacements of the wave packet by suitable modulation of the external field [14].

Also excitations (excitons) in idealized linear polymers, modeled by beads and springs, with an external field and at ultra-cold temperatures have been shown to exhibit Bloch oscillations [15]. Similar to the experiments mentioned above, one can manipulate the excitons' motion by varying the external field [16].

However, all the experiments so far consider lattice-like underlying potentials. For more complex arrangements one encounters the situation of a (quantum) graph [17, 18], where vertices are connected by arms. In order to be able to manipulate a wave packet on an arbitrary graph, one first has to understand the behavior of wave packets at bifurcation points. These points are characteristic for vertices where three (or more) arms meet. We call a graph with a single bifurcation a star graph. In the following, we will assume that each arm is modeled by a one-dimensional periodic potential and that at the vertex there is continuity and current conservation, see below.

As we will show, it is possible to manipulate a wave packet by suitable changes of the external fields. Since complex graphs can be build iteratively by joining star graphs, our results are a first step to precise manipulations of wave packets on these complex graphs. This paper is organized as follows. In the next section we will recall the problem of a tilted lattice solved in a continuous model. Section III presents the study of the directed transport in a one dimensional lattice. In section IV we

treat such transport in driven quantum star graphs. Finally, section V presents concluding remarks.

II. BLOCH OSCILLATIONS IN A ONE-DIMENSIONAL LATTICE

We start by recalling the effect of Bloch oscillations in one-dimensional periodic potentials $V(x)$. The Hamiltonian is given (in units $\hbar = 2m = 1$) by:

$$H = -\frac{\partial^2}{\partial x^2} + V(x) + fx , \tag{1}$$

where f is the external field strength and $V(x+d) = V(x)$ is the periodic potential with lattice period d. This Hamiltonian describes, for instance, an electron in a one-dimensional crystal in the presence of a constant electric field [8, 19]. Such a Hamiltonian generates time-periodic oscillations, the Bloch oscillations, of an initial Gaussian wave packet (GWP). These oscillations have a period inversely proportional to the field strength, i.e., $T_B = 2\pi\hbar/df$, and a well-defined amplitude $L = \Delta/f$, where Δ is the bandwidth. In the following we choose the lattice periodic potential as a cosine potential of the form:

$$V(x) = V_0 \cos\left(\frac{2\pi}{d}x\right) . \tag{2}$$

Exemplarily, we show in Fig. 1 the Bloch oscillations of the solution of the Schrödinger equation with H and an initial GWP over two Bloch periods. We chose the parameters such that our results are comparable to one of the discrete model discussed in Ref. [15]. We note that the solution of Eq. (1) shows the different bands of the Bloch band structure [8], while in the discrete model only the lowest band was considered. However, also for the continuous solution, the main fraction of the excitation is bounded to the lowest band, see the weak contribution of the higher bands with larger velocity in Fig. 1.
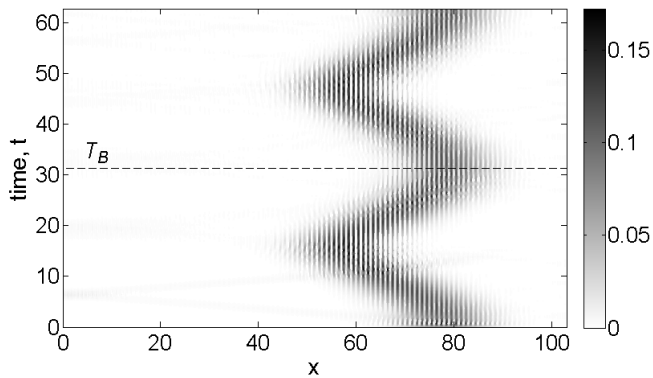
FIG. 1. Contour plot of the probability density. Bloch oscillations for $f = 0.2, d = 1$ and $V_0 = 16.7875$. One can see that the oscillation is bounded within the interval of the length $\Lambda = \Delta/f = 20$.

III. PERIODIC POTENTIALS WITH FIELD MODULATIONS

Now, modulations of the potential or of the external field allow to manipulate the motion of the GWP. In order to see this, we assume either a time-dependent potential $V(x,t)$ or a time-dependent and spatially homogeneous external field $F(t)$. Then, the Schrödinger equation in the one-dimensional case has the general form

$$i\frac{\partial}{\partial t}\Psi(x,t) = -\frac{\partial^2}{\partial x^2}\Psi(x,t) + [V(x,t) + F(t)x]\,\Psi(x,t) \;. \tag{3}$$

A simple sinusoidal change in the coupling strength is reflected by an oscillating potential amplitude leading to tunneling matrix elements of H given by

$$V(x,t) = V_0[1 - a\sin(\omega t + \phi)]\cos\left(\frac{2\pi}{d}x\right), \tag{4}$$

where $a \in [0,1]$. Fig. 2 shows three cases of the dynamics of a GWP centered at $x_0 = 78$ with a standard deviation $\sigma = 6$. Each panel displays the motion for a constant external field of strength $f = 0.2$ and an oscillating potential with parameters $d = 1$, $a = 0.85$, and $V_0 = 16.7875$, but with different phases ϕ. These parameters are such that the results match those of Ref. [15], where the oscillating coupling strength was achieved by varying distances between the centers of the (discrete) potential.

Experimentally it might be easier to modulate the external field than the potential. Thus, we consider in the following only the case of a time-dependent field $F(t) = f\sin(\omega t + \phi)$ and a time-independent periodic potential $V(x) = V_0\cos[(2\pi/d)x]$. Note, that the phase ϕ is now also shifted to the field dependence. For periodically modulated external fields, it is known from the discrete model that a GWP with an initial width σ_0 can
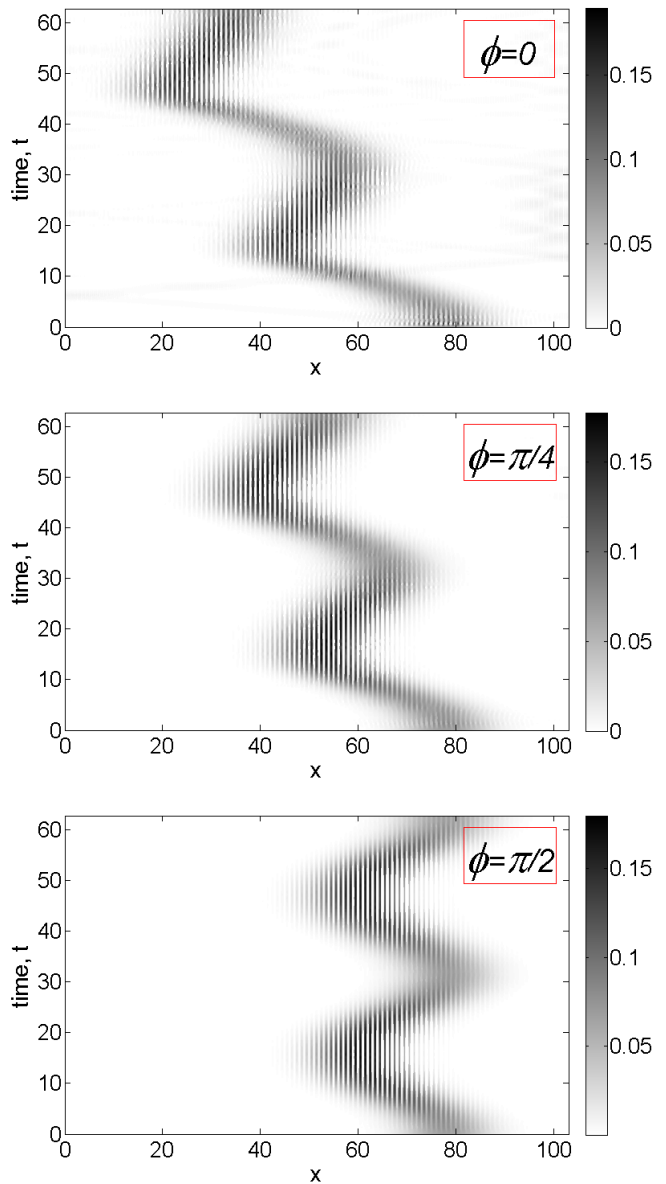

FIG. 2. Lattice potential amplitude modulation given by (4): Contour plot of probability density for $a = 0.85$ and $\omega = df$. Each plot corresponds to different values of $\phi = 0, \pi/4$ and $\pi/2$.

broaden with time [12]:

$$\sigma(t) = \sigma_0\sqrt{1 + t^2[\mathcal{J}_0(f/\omega)\cos[(f/\omega)\cos\phi]/\sigma_0^2]^2} \;, \tag{5}$$

where $\mathcal{J}_0(f/\omega)$ is the Bessel function of first kind. Therefore, whenever the Bessel function or the cosine function are zero, it is possible to preserve the width of the initial GWP, leading to a non-dispersing wave packet for a GWP with $f = \pi/10, \omega = 1/5$, and $\phi = 0$. In the following we will always use these parameters to preserve the width of the GWP (before the bifurcation point). Strictly, Eq. (5) is only valid for the lowest band, while

contributions from higher bands will in any case result in a broadening of the GWP. We confirm the preservation of the width of the GWP in the lowest band by numerical fitting to a Gaussian with parameterized width.

Fig. 3 shows the dynamics of the same initial GWP as in Fig. 2 with parameters $f = \pi/10$, $d = 1$, $\omega = 0.2$, and $V_0 = 16.7875$, for three different phases ϕ. As for the case where the potential is time-dependent, one clearly observes the ϕ-dependence of the dynamics: While for $\phi = \pi/2$ there is no net displacement after one Bloch period, one can achieve a significant displacement for $\phi = \pi/4$ and $\pi = 0$. We note, that for time-dependent fields with a phase ϕ, also the Bloch frequency depends on ϕ.

IV. DIRECTED TRANSPORT IN DRIVEN STAR GRAPH

In this section we solve the problem for a quantum star graph. Each of the arms is vested with a tilted lattice potential, and they are connected at a common (central) vertex. We assign the coordinate x to each arm, which indicates the position along the arm; x takes the value 0 at the common vertex.

Thus, we consider the time-dependent Schrödinger equation for a star graph with N arms ($\hbar = 2m = 1$):

$$i\frac{\partial}{\partial t}\Psi_j(x,t) = H_j\Psi_j(x,t), \qquad (6)$$

$$\forall t, 0 \leq x \leq L_j, \quad j = 1, ..., N$$

where

$$H_j = -\frac{\partial^2}{\partial x^2} + \left[V_0 \cos\left(\frac{2\pi}{d}x\right) + F_j(t)x\right].$$

As mentioned in the previous section, the time-dependence of the field is given by $F_j(t) = f_j \sin(\omega t + \phi_j)$, being in this case also arm-dependent, and the parameters f_j and ϕ_j are used to manipulate the GWP transition through the central vertex. The imposed conditions

$$\begin{cases} \Psi_1(L_1,t) = \Psi_2(L_2,t) = ... = \Psi_N(L_N,t) = 0 \,, \\ \Psi_1(0,t) = \Psi_2(0,t) = ... = \Psi_N(0,t) \,, \\ \sum_{j=1}^{N} \frac{\partial}{\partial x}\Psi_j(x,t)|_{x=0} = 0 \,. \end{cases} \qquad (7)$$

imply Dirichlet boundary conditions at the non-connected edges and continuity and current conservation at the vertex.

The solution of Eqs. (6)-(7) can be written in terms of the complete set of eigenfunctions $\psi_{j,n}(x)$ of the potential-free star graph:

$$\Psi_j(x,t) = \sum_n C_n(t)\psi_{j,n}(x), \quad j = 1, \ldots, N. \qquad (8)$$

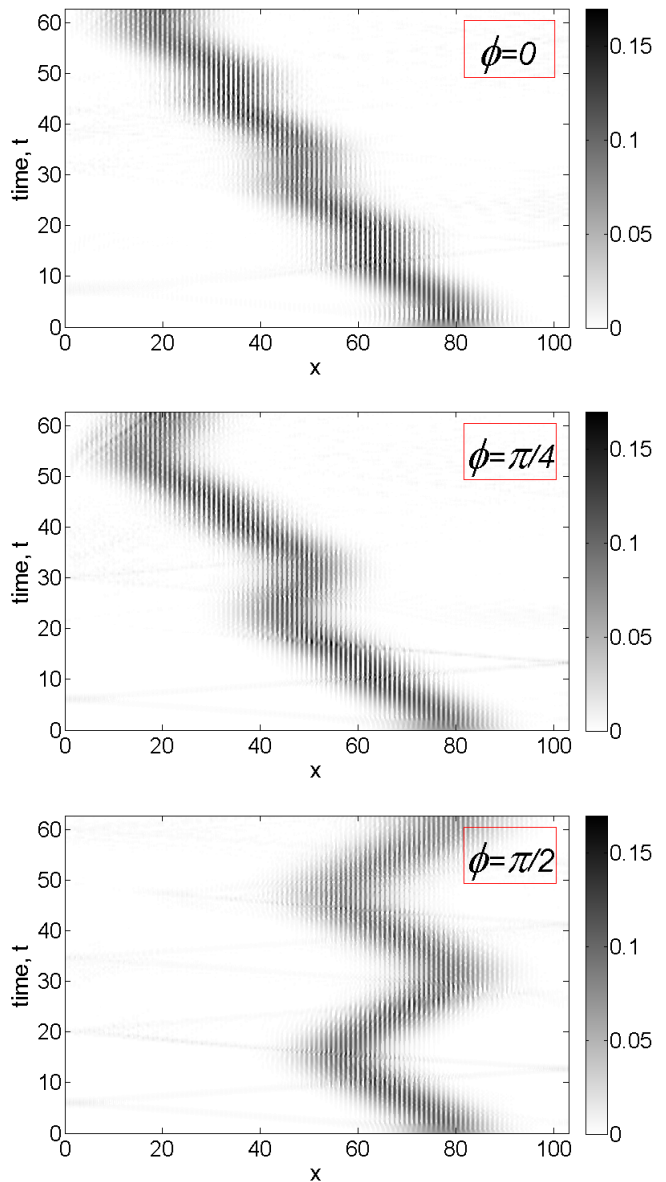where time-dependent coefficients $C_n(t)$ are to be found.

FIG. 3. The external field modulation given by $F(t) = f\sin(\omega t + \phi)$: Contour plot of probability density for $f = \pi/10$ and $\omega = 0.2$. Each plot corresponds to different values of $\phi = 0, \pi/4$ and $\pi/2$.

For the star graph with N arms the eigenfunctions $\psi_{j,n}(x)$ of the stationary Schrödinger equation (in units $\hbar = 2m = 1$):

$$-\frac{d^2}{dx^2}\psi_j(x) = k^2\psi_j(x), \quad 0 \leq x \leq L_j, \quad j = 1, ..., N, \quad (9)$$

with the same boundary conditions as in Eq. (7) have the form

$$\psi_{j,n}(x) = \frac{B_n}{\sin(k_n L_j)} \sin[k_n(L_j - x)], \qquad (10)$$

where

$$B_n = \left[\sum_j \left[L_j + \sin\left(2 k_n L_j\right) \right] \sin^{-2}\left(k_n L_j\right)/2 \right]^{-1/2} \quad (11)$$

are the normalization coefficients, and the k_n fulfill the equation:

$$\sum_{j=1}^{N} \cot(k_n L_j) = 0. \quad (12)$$

Eq. (12) can be solved numerically. In order to avoid non-generic degeneracies, the lengths of arms L_j are chosen to be rationally independent [17].

Inserting the expansion (8) into Eq. (6) and taking into

account the orthonormality of the eigenfunctions,

$$\sum_{j=1}^{N} \int_{0}^{L_j} \psi_{j,m}^* \psi_{j,n} dx = \delta_{mn}, \quad (13)$$

we get the system of ODE with respect to the coefficients:

$$i \dot{C}_n = k_n^2 C_n + \sum_m M_{nm} C_m. \quad (14)$$

The matrix M can be written in terms of the contributions arising from the lattice potential $(I^{(V)})$ and the driving external field $(I^{(F)})$:

$$M = I^{(V)} + I^{(F)},$$

the elements of which are given in Appendix A.

As the system of ODE (14) has an infinite number of equations, solving it numerically requires to limit this number. Then, to preserve the required accuracy one has to control the norm conservation condition

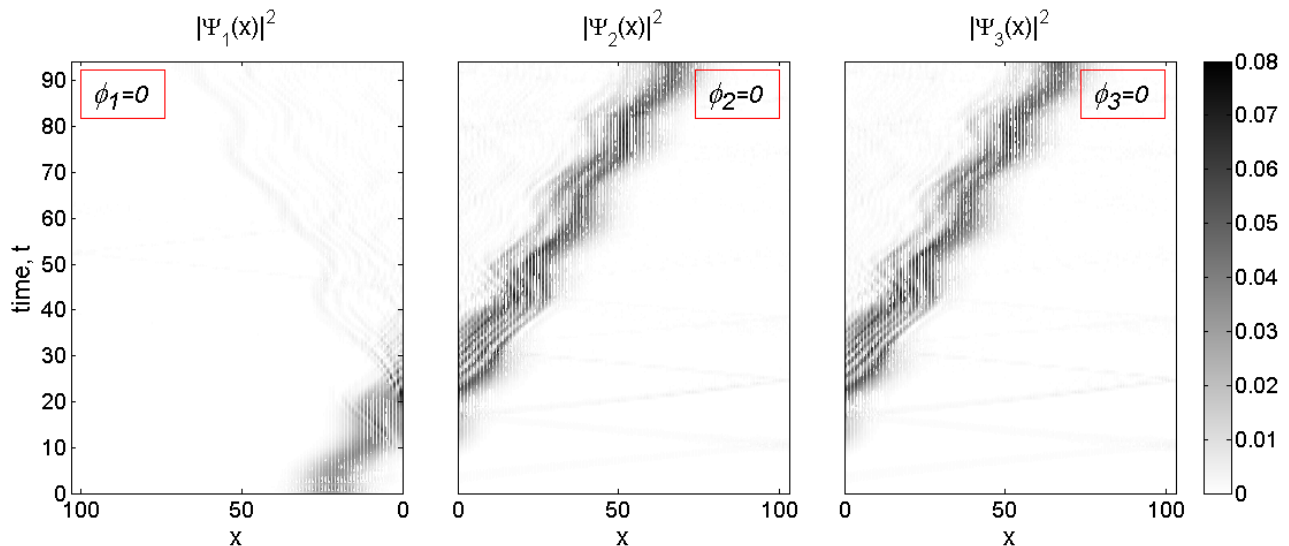$$\sum_n |C_n(t)|^2 = 1, \quad \forall t. \quad (15)$$

FIG. 4. Contour plot of the probability density for the three arm star graph, where driving external field is given by $F_j(t) = f_j \sin\left(\omega t + \phi_j\right)$ with $f_1 = -f_2 = -f_3 = \pi/10, \omega = 0.2$. The three columns correspond to the arms of the star graph. The x-coordinate of the first arm is reversed.

We now turn to the results for a GWP on a star graph. For clarity, we restrict ourselves to a star graph with three arms. Fig. 4 shows the dynamics of a GWP initially located on the first arm, at $x_0 = 22$, see the leftmost panel in Fig. 4. In this first example, the external field

strengths $F_j(t) = f_j \sin(\omega t + \phi_j)$ are of the same magnitude f for all the arms and chosen to be $f_1 = -f_2 = -f_3$, such that the field points globally in one direction. As for the case of Bloch oscillations on a single arm, the GWP moves towards the vertex (at position 0). At the
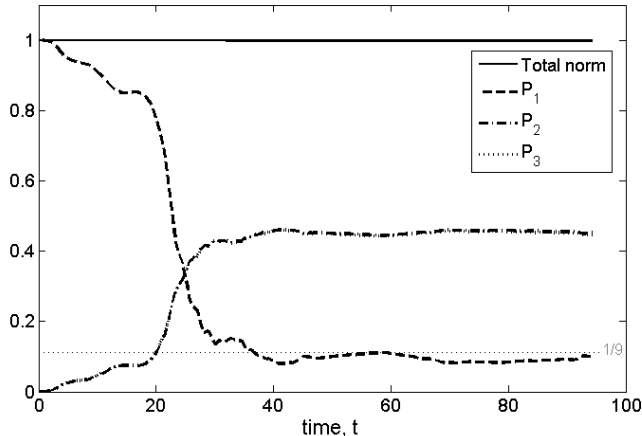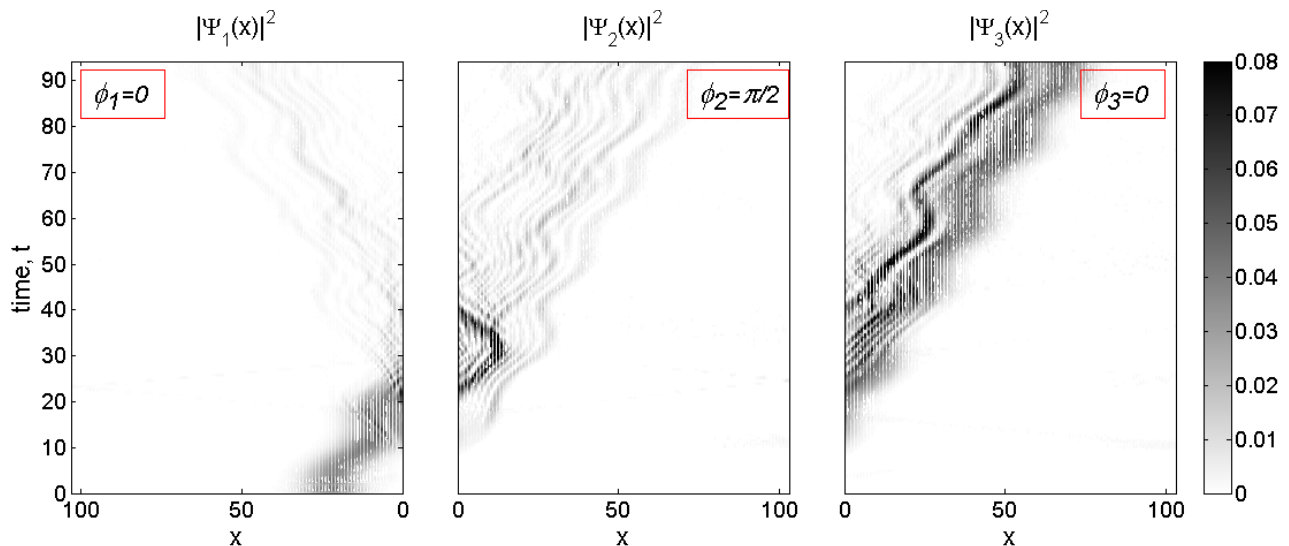
FIG. 5. The time-dependence of the partial norms corresponding to Fig. 4.

the other two arms and partly reflected back into the initial arm. As the driving external field for the second and third arms has the same parameters, the dynamics of the split GWP is identical for these two arms. This can also be seen in Fig. 5, where the time-dependence of the partial norms

$$P_j(t) = \int\limits_0^{L_j} |\Psi_j(x,t)|^2 dx, \quad j = 1, 2, .., N$$

are shown. We have confirmed that the total norm is $\sum_{j=1}^N P_j(t) = 1$. On the basis of previous results for quantum graphs with the Neumann boundary condition [17], we can calculate the fraction of the GWP which is reflected back into the initial arm as being $1/9$. The other fraction of $8/9$ of the initial GWP is split into the two identical parts. Due to the reflection and transmission at the vertex the shape of the GWP in the two arms is (slightly) distorted, but with a width which is still roughly preserved over time.

vertex the GWP bifurcates and is partly transmitted to

FIG. 6. Contour plot of the probability density for the three arm star graph, where driving external field is given by $F_j(t) = f_j \sin(\omega t + \phi_j)$ with $f_1 = -f_2 = -f_3 = \pi/10, \omega = 0.2$. The three columns correspond to the arms of the star graph. The x-coordinate of the first arm is reversed.

The situation changes when we change the phase of the second arm to $\phi_2 = \pi/2$, see Fig. 6. While the transmission into the third arm persists, although the wave packet becomes more distorted, the transmission in the second arm is nearly prohibited. This effect can be quantified by calculating the time-dependence of the partial norms, which are shown in Fig. 7. After a transient time until most reflection and transmission effects have taken place, the partial norm in arm three saturated around a value of 70%, while the partial norms of the other two arms saturate around values between 10 and 20 percent. Even though the wave packet in the third arm gets distorted it still retains a rather constant width. Therefore, by manipulating the phase of the external field in one of the arms, one is able to "block" the transmission into this arm and consequently can manipulate the direction of the initial GWP.

For our setup of initial parameters, the choice $\phi_2 = \pi/2$ turns out to be the most efficient one to realize the idea of "blocking" the wave packet propagation to the second
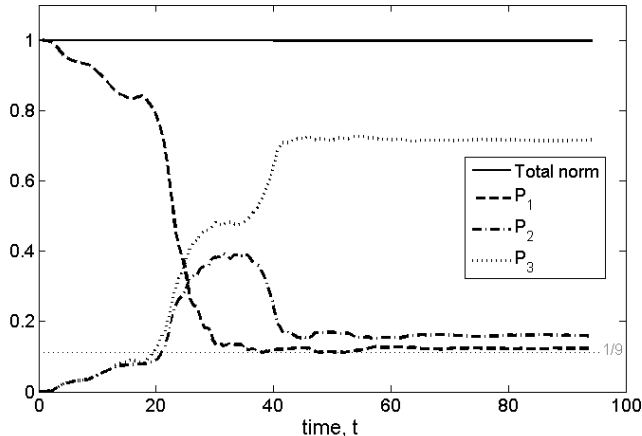
the partial norms.

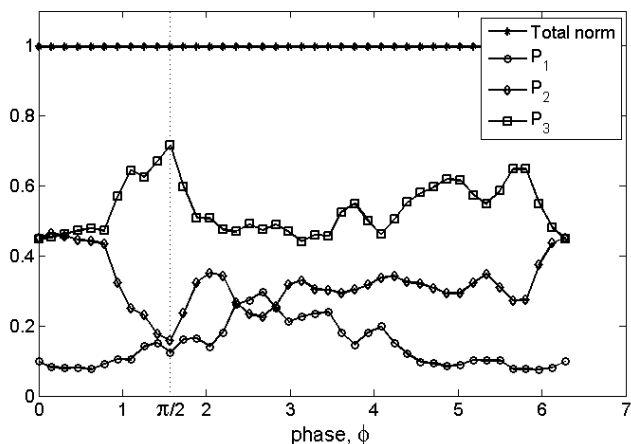FIG. 7. The time-dependence of the partial norms corresponding to Fig. 6.

FIG. 8. The phase-dependence of the partial norms at time $t = 94.25$. The external field and initial parameters correspond to Figs. 4 and 6.

arm. To show this, we calculated the partial norms for the three arms depending on the phase ϕ_2. Fig. 8 shows the value of the partial norms at times where the norms have saturated, i.e., we have chose that time at which we stop our numerical calculations, $t = 94.25$. At the value of $\phi_2 = \pi/2$, we observe the largest difference in

V. CONCLUSION

In this paper, we have investigated the possibilities of directing a Gaussian wave packet on a star graph with three arms. This can be viewed as a paradigmatic building block for complex networks, which can be composed by iteratively joining star graphs. Assuming that each arm of the graph is equipped with a periodic potential and additionally (independent) possibly time-dependent external fields act on each arm, our numerical results show that it is possible to direct a wave packet with high probability from one arm into one of the other arms while blocking the transmission into the third arm. This effect is best achieved by assuming time-periodic external fields with independent phase shifts. The phase shifts allow for a parametric tuning of the "blocking" effect. Our results further indicate that the shape of the wave packets remains almost intact. We believe that such a scenario can be realized by state-of-the-art experiments with, say, ultra-cold atoms in optical lattices. One can also imagine that after transmission of the wave packet into one arm, the shape of the wave packet can be re-established, see, e.g., [20]. The fact that there is not perfect transfer into the desired arm can be explained by fundamental reflection and transmission rules at the bifurcation point, see also [17]. This study being a proof of concept, we will extend our analysis to more complex situations where several star graphs are joined together forming more complex networks, such as, e.g., T-fractals [21] or dendrimers [22].

Appendix A: Calculation of matrices $I^{(V)}$ and $I^{(F)}$

The elements of the matrices $I^{(V)}$ and $I^{(F)}$ have integral forms, which can be solved analytically. Denoting the frequency of the periodical lattice potential by $\omega_d = 2\pi/d$ one gets the following:

$$I_{nm}^{(V)} = V_0 \sum_{j=1}^{N} \int_0^{L_j} \psi_{j,m}^* \cos{(\omega_d x)} \psi_{j,n} dx \tag{A1}$$

$$= V_0 \sum_{j=1}^{N} \frac{B_n B_m}{4 \sin{(k_n L_j)} \sin{(k_m L_j)}} \left[\frac{\sin{(\omega_d L_j)} + \sin{(k_n - k_m)L_j}}{\omega_d + k_n - k_m} + \frac{\sin{(\omega_d L_j)} - \sin{(k_n - k_m)L_j}}{\omega_d - k_n + k_m} \right.$$
$$\left. - \frac{\sin{(\omega_d L_j)} + \sin{(k_n + k_m)L_j}}{\omega_d + k_n + k_m} - \frac{\sin{(\omega_d L_j)} - \sin{(k_n + k_m)L_j}}{\omega_d - k_n - k_m} \right],$$

$$I_{nm}^{(F)} = \sum_{j=1}^{N} F_j(t) \int_0^{L_j} \psi_{j,m}^* x \psi_{j,n} dx = \sum_{j=1}^{N} \frac{F_j(t) B_n B_m}{\sin{(k_n L_j)} \sin{(k_m L_j)}} A_{nm}, \tag{A2}$$

where the diagonal elements of matrix A (i.e. for $m = n$) are:

$$A_{nn} = \frac{L_j^2}{2} - \frac{1 - \cos{(2 k_n L_j)}}{4 k_n^2}$$

and the off-diagonal elements $(m \neq n)$ are:

$$A_{nm} = \frac{1 - \cos 2(k_n - k_m)L_j}{(k_n - k_m)^2} - \frac{1 - \cos 2(k_n + k_m)L_j}{(k_n + k_m)^2}.$$

[1] I. Bloch, Nature Phys. **1**, 23 (2005).
[2] A. Szameit and S. Nolte, J. Phys. B **43**, 163001 (2010).
[3] A. Block, C. Etrich, T. Limboeck, F. Bleckmann, E. Soergel, C. Rockstuhl, and S. Linden, Nature Commun. **5** (2014).
[4] T. Dekorsy, R. Ott, H. Kurz, and K. Köhler, Phys. Rev. B **51**, 17275 (1995).
[5] M. Ben Dahan, E. Peik, J. Reichel, Y. Castin, and C. Salomon, Phys. Rev. Lett. **76**, 4508 (1996).
[6] E. Haller, R. Hart, M. J. Mark, J. G. Danzl, L. Reichsöllner, and H.-C. Nägerl, Phys. Rev. Lett. **104**, 200403 (2010).
[7] J. S. Lehtinen, K. Zakharov, and K. Y. Arutyunov, Phys. Rev. Lett. **109**, 187001 (2012).
[8] T. Hartmann, F. Keck, H. J. Korsch, and S. Mossmann, New J. Phys. **6**, 2 (2004).
[9] B. M. Breid, D. Witthaut, and H. J. Korsch, New J. Phys. **9**, 62 (2007).
[10] Q. Thommen, J. C. Garreau, and V. Zehnlé, J. Opt. B **6**, 301 (2004).
[11] S. Arlinghaus and M. Holthaus, Phys. Rev. A **84**, 063617 (2011).
[12] C. E. Creffield and F. Sols, Phys. Rev. A **84**, 023630 (2011).
[13] W. Hu, L. Jin, and Z. Song, Quantum Inf. Process. **12**, 3569 (2013).
[14] Q. Thommen, J. C. Garreau, and V. Zehnlé, Phys. Rev. A **84**, 043403 (2011).
[15] O. Mülken and M. Bauer, Phys. Rev. E **83**, 061123 (2011).
[16] Q. Thommen, J. C. Garreau, and V. Zehnlé, Phys. Rev. A **65**, 053406 (2002).
[17] T. Kottos and U. Smilansky, Ann. Phys. **274**, 76 (1999).
[18] S. Gnutzmann and U. Smilansky, Adv. Phys. **55**, 527 (2006).
[19] M. Glück, A. R. Kolovsky, and H. J. Korsch, Phys. Rep. **366**, 103 (2002).
[20] R. Uberna, Z. Amitay, R. A. Loomis, and S. R. Leone, Faraday Discussions **113**, 385 (1999).
[21] E. Agliari, Phys. Rev. E **77**, 011128 (2008).
[22] O. Mülken, V. Bierbaum, and A. Blumen, J. Chem. Phys. **124**, 124905 (2006).